

# Role of $^{18}\text{F}$ -FDG PET/CT in Large Vessel Vasculitis and Polymyalgia Rheumatica

Riemer H.J.A. Slart<sup>1,2</sup>, Pieter H. Nienhuis<sup>1,3</sup>, Andor W.J.M. Glaudemans<sup>1</sup>, Elisabeth Brouwer<sup>3</sup>, Olivier Gheysens<sup>4</sup>, and Kornelis S.M. van der Geest<sup>3</sup>

<sup>1</sup>Medical Imaging Center, Department of Nuclear Medicine and Molecular Imaging, University Medical Center Groningen, University of Groningen, The Netherlands; <sup>2</sup>Department of Biomedical Photonic Imaging, Faculty of Science and Technology, University of Twente, Enschede, The Netherlands; <sup>3</sup>Department of Rheumatology and Clinical Immunology, University Medical Center Groningen, University of Groningen, The Netherlands; and <sup>4</sup>Department of Nuclear Medicine, Cliniques Universitaires Saint-Luc and Institute of Clinical and Experimental Research, Université Catholique de Louvain, Brussels, Belgium

**Learning Objectives:** On successful completion of this activity, participants should be able to (1) understand the role of  $^{18}\text{F}$ -FDG PET/CT for diagnosis and therapy monitoring of LVV and PMR; (2) learn about the strengths and limitations of  $^{18}\text{F}$ -FDG PET/CT in LVV and PMR, including the pitfalls; (3) know the PET procedures around LVV and PMR; and (4) realize the potential of more specific PET tracers in LVV and PMR, particularly in monitoring disease activity.

**Financial Disclosure:** Kornelis van der Geest received a speaker fee from Roche and research support from AbbVie. In accordance with ACCME Revised Standards for Commercial Support and SNMMI Conflict-of-Interest Policy, the authors have indicated no other relevant relationships that could be perceived as a real or apparent conflict of interest. Disclosure of a relationship is not intended to suggest or to condone bias but is made to provide participants with information that might be of potential importance to their evaluation of the activity.

**CME Credit:** SNMMI is accredited by the Accreditation Council for Continuing Medical Education (ACCME) to sponsor continuing education for physicians. SNMMI designates each *JNM* continuing education article for a maximum of 2.0 AMA PRA Category 1 Credits. Physicians should claim only credit commensurate with the extent of their participation in the activity. For CE credit, SAM, and other credit types, participants can access this activity through the SNMMI website (<http://www.snmmilearningcenter.org>) through April 2026.

Systemic vasculitides comprise a group of autoimmune diseases affecting blood vessels, including large vessel vasculitis (LVV) and medium-sized vessel vasculitis such as giant cell arteritis (GCA) and Takayasu arteritis (TAK). GCA frequently overlaps with polymyalgia rheumatica (PMR), a rheumatic inflammatory condition affecting bursae, tendons or tendon sheaths, and joints.  $^{18}\text{F}$ -FDG PET/CT plays an important role in the diagnostic work-up of GCA, PMR, and TAK and is increasingly used to monitor treatment response. This continuing education article provides up-to-date guidance on the role of  $^{18}\text{F}$ -FDG PET/CT in patients with LVV, medium-sized vessel vasculitis, and PMR. It provides a general introduction on the clinical presentation and challenges in the diagnostic work-up of LVV and medium-sized vessel vasculitis, with a focus on the 2 major LVV subtypes: GCA, including PMR, and TAK. Next, practice points to perform and interpret the results of  $^{18}\text{F}$ -FDG PET/CT are described in line with the published procedure recommendations. Furthermore, the diagnostic performance and its role for treatment monitoring are discussed, taking into account recent international recommendations for the use of imaging in LVV and medium-sized vessel vasculitis in clinical practice. This is illustrated by several clinically representative PET/CT scan examples. Lastly, knowledge of limitations and pitfalls is essential to understand the role of  $^{18}\text{F}$ -FDG PET/CT in LVV, medium-sized vessel vasculitis, and PMR. Challenges and opportunities, as well as future research and conclusions, are highlighted. Learning objectives provide up-to-date guidance for the role of  $^{18}\text{F}$ -FDG PET/CT in patients with suspected LVV, medium-sized vessel vasculitis, and PMR.

**Key Words:** large vessel vasculitis; cranial GCA; PMR;  $^{18}\text{F}$ -FDG PET/CT; procedures

**J Nucl Med 2023; 64:515–521**

DOI: 10.2967/jnumed.122.265016

The autoimmune vasculitides encompass a heterogeneous group of diseases characterized by inflammation of blood vessels. Classification is based on the size and the type of vessels that are preferentially affected by the specific type of vasculitis (1). The main forms of large vessel vasculitis (LVV) include giant cell arteritis (GCA) and Takayasu arteritis (TAK). GCA is the most common form of vasculitis in European populations, with the highest lifetime risk (i.e., 0.5%–1%) among people of Northern European descent (Figs. 1 and 2) (2). In contrast, TAK is more common in Asian populations (Fig. 3) (3). GCA and TAK more often affect women. One important distinction between GCA and TAK is the age of disease onset. TAK primarily occurs before the age of 40, whereas GCA affects individuals after the age of 50, with a mean age between 70–75 y (Fig. 4). Furthermore, GCA frequently overlaps with polymyalgia rheumatica (PMR), a rheumatic inflammatory condition affecting bursae, tendons or tendon sheaths, and joints (Fig. 5) (4–6). PMR may also occur in the absence of GCA and is the most common rheumatic inflammatory condition in the elderly, with an age distribution similar to that of GCA (2).

Historically, involvement of cranial arteries was thought to be a hallmark of GCA. This is reflected in one of the earlier names of the disease, temporal arteritis, and the American College of Rheumatology 1990 criteria for the classification of GCA, which focused on cranial symptoms and signs and biopsy proof of temporal artery inflammation. This cranial GCA (C-GCA) may give rise to classic symptoms such as headache, jaw claudication, and ischemic visual loss (7), the latter reflecting infarction of the optic nerve related to inflammation of the posterior ciliary arteries (8). With the emerging role of imaging, it has been recognized that

Received Dec. 21, 2022; revision accepted Feb. 2, 2023.

For correspondence or reprints, contact Riemer H.J.A. Slart (r.h.j.a.slart@umcg.nl).

COPYRIGHT © 2023 by the Society of Nuclear Medicine and Molecular Imaging.

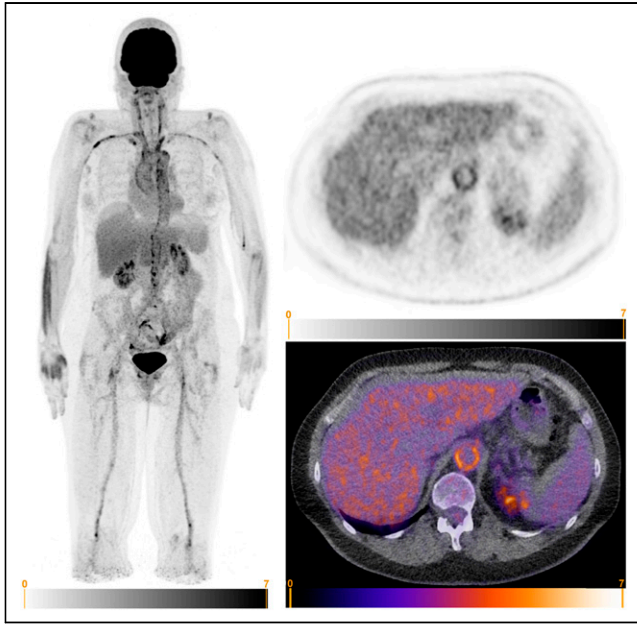


**FIGURE 1.** Digital  $^{18}\text{F}$ -FDG PET/CT of 64-y-old female with suspected GCA. Patient presented with fatigue and claudication of arms. Measurements of systolic blood pressure in brachial arteries varied significantly. Measurements lower than 100 mm Hg and higher than 120 mm Hg were sequentially registered. Duplex ultrasonography showed bilateral stenosis of subclavian and axillary arteries. Patient also complained of morning stiffness and pain in neck, shoulders, and hips. (Left) Maximum-intensity-projection  $^{18}\text{F}$ -FDG PET image showing significantly increased uptake (higher than liver) in aorta, carotid, subclavian, and axillary arteries. Increased uptake (similar to liver) may also be seen in femoral and popliteal arteries, as well as around hips and shoulders. (Right bottom) Axial fused  $^{18}\text{F}$ -FDG PET/CT images showing significantly increased uptake in suprarenal abdominal aorta. Diffuse and circular uptake is highly suggestive of LVV.

many patients with GCA may also have inflammation of the aorta and its major branches and that this large vessel involvement can occur in the absence of cranial artery involvement (9). Consequently, clinicians now classify C-GCA and large vessel GCA (LV-GCA) according to symptoms or affected arteries on imaging (10).

In general, TAK can affect the same vasculature as LV-GCA, although some differences exist. For instance, carotid, mesenteric, and renal artery involvement is more common in TAK. In contrast, temporal artery involvement is less common in TAK, and involvement of the ocular arterial system is rare (11). Patients with LV-GCA or TAK may present with fever of unknown origin, but more specific symptoms such as arm claudication and carotidynia can occur (7,11). Aortitis is an all-encompassing term ascribed to inflammation solely of the aorta (Fig. 6). It includes “true” aortitis limited to the vascular wall and periaortitis and involving the adventitial layer and potentially surrounding fat and other soft tissues. Periaortitis may also present as an inflammatory aneurysm or retroperitoneal fibrosis.

In all vasculitides, laboratory testing usually shows raised inflammatory markers in the blood. C-GCA can be further demonstrated by temporal artery biopsy, color Doppler ultrasonography (CDUS) of the superficial vessels, and MR angiography (MRA), with recent clinical guidelines suggesting a prominent role of CDUS as a first-line test in suspected C-GCA (12). MRA, CT angiography (CTA), and CDUS can be used for detection of vascular inflammation in LV-GCA and TAK (12). Ultrasonography and MRI of the shoulder

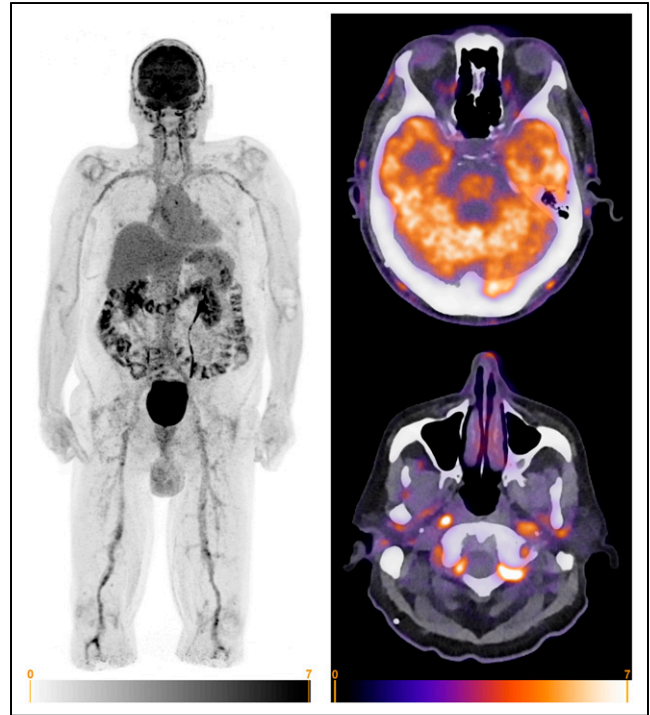


**FIGURE 2.** Digital  $^{18}\text{F}$ -FDG PET/CT of 80-y-old male with suspected GCA. Patient’s main symptom consisted of both-sided temporal headache, which was accompanied by fatigue. Laboratory investigation showed C-reactive protein of 120 mg/L. (Left) Maximum-intensity-projection  $^{18}\text{F}$ -FDG PET image showing strongly elevated uptake (significantly higher than background) in cranial arteries, most notably in superficial temporal and carotid arteries. Elevated uptake (similar to liver uptake) can be seen in subclavian, axillary, femoral, and popliteal arteries. These findings are highly suggestive of C-GCA and LV-GCA. In addition, moderate uptake can be seen around shoulders and hips, suspected for PMR activity. (Right) Axial  $^{18}\text{F}$ -FDG PET/CT fusion images of head. (Right top) Elevated uptake in frontal and parietal branches of superficial temporal artery, left posterior auricular artery, and occipital arteries. (Right bottom) Significantly increased uptake in internal carotid and vertebral arteries. Elevated uptake can also be seen at junction of external carotid artery and common superficial temporal artery, as well as maxillary arteries and right posterior deep temporal artery.

and hip girdle may demonstrate inflammation of bursae, tendons or tendon sheaths, and joints in patients with PMR (13–15). In addition,  $^{18}\text{F}$ -FDG PET/CT is considered an important tool to demonstrate inflammation in GCA, PMR, and TAK.

Glucocorticoid (GC) treatment is the cornerstone in GCA, PMR, and TAK. High initial GC doses are used in GCA and TAK: typically 40–60 mg of prednisone daily, with 500- to 1,000-mg methylprednisolone pulse therapy on 3 consecutive days reserved for patients with severe ischemic manifestations (e.g., visual loss) (16). In TAK, the clinical guidelines indicate that GC treatment should be combined with other immunosuppressive agents early in the disease. First-line treatment of TAK may consist of conventional synthetic disease-modifying antirheumatic drugs, such as methotrexate and azathioprine (16,17). Anti-TNF and anti-IL-6 receptor therapy may serve as second-line immunosuppressive therapy in refractory and relapsing cases. Treatment guidelines for GCA by the American College of Rheumatology suggest early initiation of anti-IL-6 receptor therapy in all newly diagnosed patients (18), whereas European League Against Rheumatism recommendations advocate the addition of anti-IL-6R



**FIGURE 3.**  $^{18}\text{F}$ -FDG PET/CT of 16-y-old female with suspected TAK. Patient had been experiencing generalized malaise. Laboratory investigations showed C-reactive protein of 98 mg/L and ESR of 119 mm/h. Maximum-intensity-projection  $^{18}\text{F}$ -FDG PET image shows elevated uptake in thoracic aorta and part of abdominal aorta. ESR = erythrocyte sedimentation rate.

therapy in cases of relative contraindications for GC treatment or a relapsing disease course (16). Methotrexate is considered a reasonable alternative for anti-IL-6 receptor therapy, according to American College of Rheumatology guidelines and European League Against Rheumatism recommendations. Patients with PMR are typically started on medium GC doses (15 mg of prednisone) daily (19). GC-sparing immunosuppressants such as methotrexate are usually added when patients with PMR suffer from GC side effects or disease relapse.

#### **ROLE OF $^{18}\text{F}$ -FDG PET/CT ANGIOGRAPHY (PET/CT[A]) IN DIAGNOSING LJV AND PMR**

Ultrasonography and MRA are mainly used to detect C-GCA, whereas CTA, MRA, and  $^{18}\text{F}$ -FDG PET/CT are useful

for detecting LV-GCA in patients presenting with general symptoms (12). However, the new-generation PET/CT scanners, providing superior sensitivity and better spatial resolution, also allows visualization of the cranial arteries by  $^{18}\text{F}$ -FDG PET/CT (20,21).  $^{18}\text{F}$ -FDG PET/CT can be used in patients with clinical symptoms of C-GCA, LV-GCA, and TAK to visualize which vessels are involved, disease extent and activity, and coexistence of PMR.  $^{18}\text{F}$ -FDG PET/CT can also be used in patients without typical clinical symptoms but with persisting fever or inflammation of unknown origin. Vasculitis or PMR can be one of the diseases causing this inflammation or fever.

Normally, low-dose CT is performed in PET imaging for attenuation correction and anatomic localization. However, performing contrast-enhanced CT is also possible according to local practice or guidelines, and newer PET/CT camera systems offer the possibility to perform a CTA directly after the PET acquisition and with the same quality as performed on a single CT camera system. Therefore, PET/CTA combines the unique characteristics of the PET part in visualizing the metabolic activity of the vessel walls and the CTA characteristics of visualizing anatomic changes or stenoses of the vessels in a single imaging modality.

In GCA, a prospective study of  $^{18}\text{F}$ -FDG PET imaging in patients with GCA showed vascular  $^{18}\text{F}$ -FDG uptake in 83% of patients, particularly at the subclavian arteries (74%) but also in the thoracic and abdominal aorta (>50%) and the femoral arteries (37%) (22). A metaanalysis of 6 studies evaluating  $^{18}\text{F}$ -FDG PET for the diagnosis of GCA reported an overall sensitivity of 80% and specificity of 89%. Moreover, the negative predictive value of a  $^{18}\text{F}$ -FDG PET scan for GCA was excellent (88%) (23).

$^{18}\text{F}$ -FDG PET/CT is also widely used for the diagnosis of TAK (24). One metaanalysis, including patients with TAK, reported a sensitivity of 81% and specificity of 74% for  $^{18}\text{F}$ -FDG PET/CT (25). For diagnosing C-GCA, a binary visual  $^{18}\text{F}$ -FDG uptake score has been proposed that yields a sensitivity of 73%–83% and specificity of 75%–100% (20,21,26).

$^{18}\text{F}$ -FDG PET/CT is an accurate imaging method for distinguishing between aortitis and periaortitis, which is important for identifying the underlying cause (e.g., infectious and noninfectious conditions) (27,28). Mild and heterogeneous metabolic activity of the aortic wall is frequently noticed in the absence of vasculitis, especially in atherosclerotic aneurysms (29). Periaortitis is characterized by a periaortic soft-tissue mass surrounding the aorta and eccentric to the calcifications of the media, visible on radiographic imaging and ultrasound.  $^{18}\text{F}$ -FDG uptake is an important indicator of active disease, potentially enabling (treatment) follow-up (30).

$^{18}\text{F}$ -FDG PET/CT can also show inflammation of periarticular and articular synovial structures in overlapping PMR or in isolated PMR. Van der Geest et al. (31) demonstrated in a systematic review that

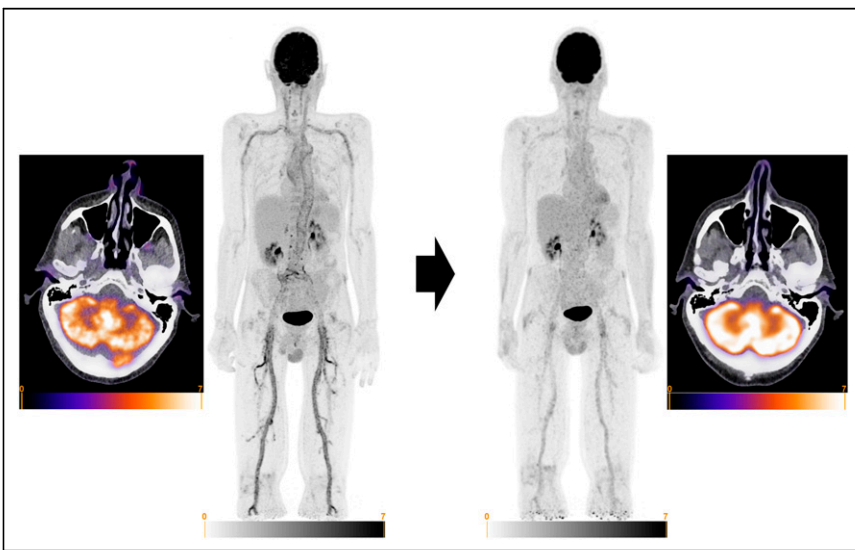


**FIGURE 4.**  $^{18}\text{F}$ -FDG PET/CT imaging at time of diagnosis (before treatment) and after 1 y of treatment in 67-y-old male GCA patient. At time of diagnosis, patient presented with complaints of PMR, accompanied by C-reactive protein (CRP) of 121 mg/L and ESR of 106 mm/h. Patient had been treated with prednisolone and subsequently with methotrexate. At 1 y, CRP remained elevated despite methotrexate treatment. Patient did not experience GCA-related symptoms at that time but had some symptoms of PMR. (Left) Axial  $^{18}\text{F}$ -FDG PET/CT fusion image of head and whole-body maximum-intensity-projection (MIP) image at time of diagnosis. Moderately increased uptake (higher than background) can be seen in maxillary arteries. Significantly increased uptake (higher than liver) can also be found in aorta and carotid, subclavian, axillary, iliac, and femoral arteries (PETVAS = 27). In addition, moderately increased uptake (similar to liver) can be observed surrounding shoulders and hips. (Right) Whole-body MIP image and axial  $^{18}\text{F}$ -FDG PET/CT fusion of head after 1 y of treatment. Slightly increased uptake (similar to liver) can be observed in aorta and carotid, subclavian, axillary, iliac, and femoral arteries (PETVAS = 13). No uptake was found in maxillary arteries. Moderately increased uptake was found surrounding hip joints. ESR = erythrocyte sedimentation rate.

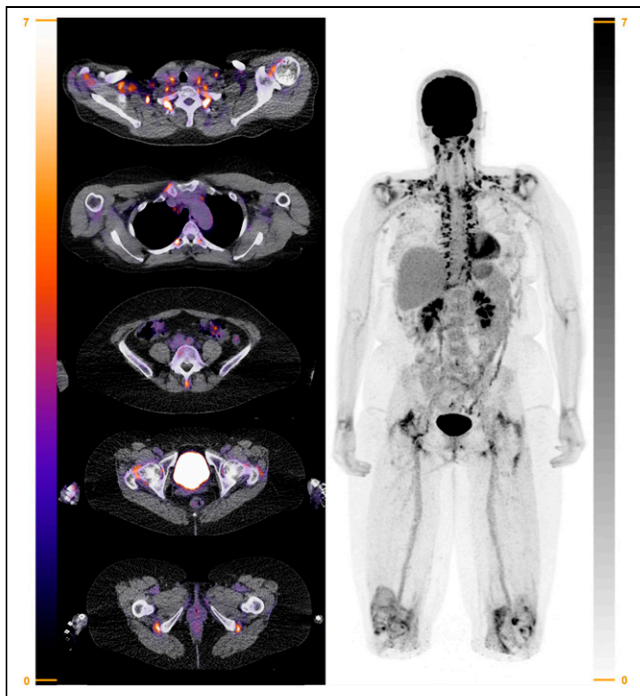


**FIGURE 5.** Digital  $^{18}\text{F}$ -FDG PET/CT in 59-y-old female patient suspected of having PMR. Patient presented at rheumatology outpatient clinic with pain in neck, shoulders, and hips. She also experienced morning stiffness of 2 h, and her blood inflammatory markers were increased (C-reactive protein, 63 mg/L; ESR, 72 mm/h). (Left) Axial  $^{18}\text{F}$ -FDG PET/CT fusion images showing significantly increased uptake (higher than liver) in shoulders, right sternoclavicular joint, lumbar interspinous bursa, hips, and ischial tuberosities. (Right) Whole-body maximum-intensity-projection image showing significantly increased  $^{18}\text{F}$ -FDG uptake in shoulders, sternoclavicular joints, lumbar interspinous bursa, hips, ischial tuberosities, and knees. Slightly elevated  $^{18}\text{F}$ -FDG uptake may be seen in wrists. Increased  $^{18}\text{F}$ -FDG uptake due to brown fat activation can also be seen in neck and paravertebral at thoracic spine (Leuven score = 23, Groningen/Leuven score = 14) (Supplemental Table 1). ESR = erythrocyte sedimentation rate.

$^{18}\text{F}$ -FDG uptake at multiple anatomic sites in the shoulder and hip girdle and spinal column is informative for a diagnosis of PMR.

#### ROLE OF $^{18}\text{F}$ -FDG PET/CT(A) IN THERAPY MONITORING OF LVV AND PMR

Therapeutic monitoring can be challenging in patients with LVV and PMR, because signs and symptoms and laboratory tests are not specific for these conditions. In addition, inflammatory markers in the blood are often lower during relapse than at diagnosis (32). Imaging tools could thus be of interest for monitoring disease activity during treatment.

Currently,  $^{18}\text{F}$ -FDG PET/CT is not routinely recommended for treatment monitoring in GCA and PMR in clinical routine (33). Even though high-dose GC treatment has substantial effects on  $^{18}\text{F}$ -FDG uptake after 10 d of treatment (34), it seems that some arterial wall  $^{18}\text{F}$ -FDG uptake may persist during treatment-induced remission later in the disease course (35). Nevertheless, most studies show that the extent and intensity of  $^{18}\text{F}$ -FDG uptake decrease during treatment. Hence, a metaanalysis suggested that  $^{18}\text{F}$ -FDG PET/CT has a moderate sensitivity of 78% and specificity of 71% for distinguishing active from quiescent LV-GCA during treatment (24). A comparable diagnostic accuracy was

noted in a recent study with 100 consecutive LV-GCA patients (36). The treatment effect on arterial wall uptake is not restricted to GC treatment, but a similar decrease has been observed in GCA patients treated with methotrexate and anti-IL-6 receptor therapy (37).

Few studies have examined the potential role of  $^{18}\text{F}$ -FDG PET/CT for treatment monitoring of PMR, because response to treatment is usually based on a clinical evaluation (38,39). Comparable to arterial wall  $^{18}\text{F}$ -FDG uptake in LVV, studies in PMR patients have shown that  $^{18}\text{F}$ -FDG uptake at the shoulder and pelvic girdle and interspinous bursae decreases, but not necessarily normalizes, during treatment-induced remission (31).

#### PET PROCEDURES

##### Patient Preparation and Scan Acquisition

Optimal patient preparation is crucial (Table 1). Patients must be fasting for at least 6 h and avoid strenuous activity for 24 h before  $^{18}\text{F}$ -FDG injection. Blood glucose levels are preferably less than 7 mmol/L.  $^{18}\text{F}$ -FDG PET should be performed before GC treatment (unless there is a risk of ischemic complications) or within the first 3 d of treatment. For PET/CT acquisition, low-dose, non-contrast-enhanced CT (for attenuation correction and anatomic reference) is performed from the vertex to the feet (or at least including the knees) 60 min after  $^{18}\text{F}$ -FDG injection, with the patient in a supine position with the arms next to the body. It is described that a time interval of 2 h may be even more optimal for PET activity detection in GCA (40). Injected activities, scan duration, or diagnostic contrast-enhanced CT may be performed according to applicable local protocols and guidelines (33).

##### Scan Interpretation and $^{18}\text{F}$ -FDG PET/CT Scores

Several  $^{18}\text{F}$ -FDG PET interpretation criteria, both visual and semi-quantitative, have been proposed, and there is insufficient evidence that semiquantitative parameters may outperform a visual grading scale to diagnose LVV in routine clinical practice (41). A standardized 4-point visual grading scale (arterial to liver uptake) is recommended with grade 0, no uptake; grade 1, uptake lower than liver; grade 2, uptake similar to liver; and grade 3, uptake higher than liver. Grade 3 is considered positive for LVV, whereas grade 2 may be indicative of LVV (33). In addition, a quantitative composite score, based on the visual grading scale of several individual arterial segments (typically between 7 and 15 segments), could be applied that is known as the total vascular score or PET vascular activity score (PETVAS) (33,42,43). This composite score provides an overall assessment of disease burden, has proven robust with little interobserver variability, and may be preferred for evaluating treatment response.  $^{18}\text{F}$ -FDG uptake in cranial arteries are scored as 3-point visual grading (0–2), with grade 0 representing uptake not above the surrounding tissue, grade 1 representing uptake just above the surrounding tissue, and grade 2 representing uptake significantly above the surrounding tissue (21).

In PMR, various  $^{18}\text{F}$ -FDG PET scores have been reported. The Leuven score is the best validated one, providing a pooled sensitivity of 89.6% and specificity of 93.3% (Supplemental Table 1) (supplemental materials are available at <http://jnm.snmjournals.org>) (44–46). The Leuven score is the summed score of visual  $^{18}\text{F}$ -FDG uptake at the cervical and lumbar interspinous bursae, sternoclavicular joints, ischial tuberosities, greater trochanters, hips, and shoulders (44).  $^{18}\text{F}$ -FDG uptake is graded according to a standardized 3-point visual  $^{18}\text{F}$ -FDG grading scale: grade 0, no uptake; grade 1, uptake lower than liver; and grade 2, uptake similar to or higher

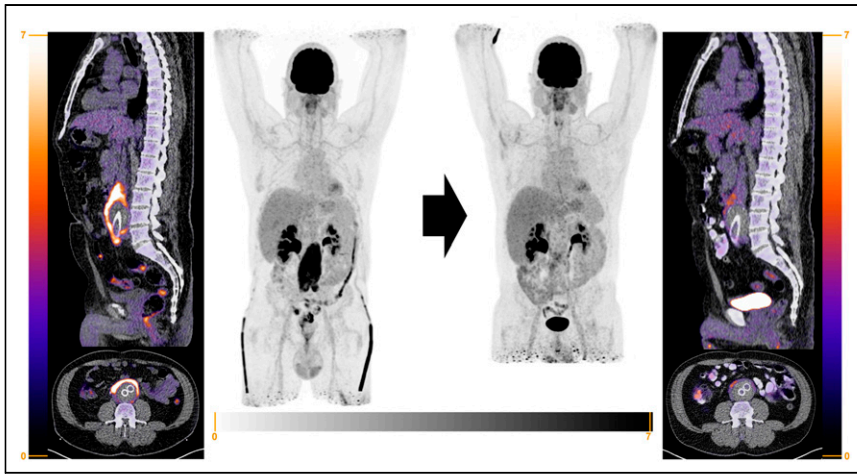


**FIGURE 6.**  $^{18}\text{F}$ -FDG PET/CT of 52-y-old man with history of idiopathic inflammatory abdominal aortic aneurysm for which he underwent prosthetic vascular graft surgery. Patient presented 1 y after surgery with increased C-reactive protein (231 mg/L) and decreased kidney function based on post-renal obstruction. Patient was diagnosed with recurrence of inflammatory aneurysm and received therapy with high-dose GCs and azathioprine. Ureteric obstruction was treated with temporary nephrostomy catheters. Immunosuppressive therapy was tapered in following 2 y. No clinical or biochemical signs of active (peri-)aortitis recurred. (Left) Sagittal and axial  $^{18}\text{F}$ -FDG PET/CT fusion images and whole-body maximum-intensity-projection (MIP) image of patient at time of diagnosis (before starting immunosuppressive treatment). Markedly increased, diffuse, and circular  $^{18}\text{F}$ -FDG uptake is seen in dilated aortic wall. There is no evidence of inflammatory activity in other locations, including prosthetic graft itself. Right: whole-body MIP image and sagittal and axial  $^{18}\text{F}$ -FDG PET/CT fusion images of patient 2 y later after withdrawal of GC therapy.  $^{18}\text{F}$ -FDG uptake was significantly decreased compared with time of diagnosis but had not completely normalized.

than liver. A concise version, the Leuven/Groningen score, appears to be at least equally informative for a diagnosis of PMR, only requiring visual assessment of  $^{18}\text{F}$ -FDG uptake at the sternoclavicular joints, hips, ischial tuberosities, and lumbar interspinous bursa (45,46). The Leuven and Leuven/Groningen scores also provide excellent interrater agreement (46).

#### Pitfalls

Blood glucose levels should be as low as possible (preferably  $<7$  mmol/L). Even though hyperglycemia may not have a significant impact on the false-negative rate of  $^{18}\text{F}$ -FDG PET for detecting inflammatory lesions (in contrast to oncologic indications), a negative correlation has been observed between blood glucose levels and  $^{18}\text{F}$ -FDG arterial wall uptake (47,48).

rather reflects a chronic, low-grade, nonspecific reaction to the graft material (51).

#### CHALLENGES FOR THE FUTURE AND CONCLUSIONS

Although  $^{18}\text{F}$ -FDG PET/CT has become an important diagnostic test in the evaluation of LVV and PMR, various questions regarding its use in LVV and PMR warrant further research. Standardization of  $^{18}\text{F}$ -FDG PET/CT scans is crucial, including the complete PET procedure, patient preparation, scan acquisition, scan reconstruction, and image analysis, and standards should be followed and adapted when needed (33). Development of scoring methods for PMR activity on PET is ongoing, and these methods need to be validated in large, prospective cohort studies. Developments in PET/CT camera

**TABLE 1**  
Patient Preparation and  $^{18}\text{F}$ -FDG PET/CT Acquisition

Preparation	Acquisition
Dietary preparation	Fast for $\geq 6$ h before $^{18}\text{F}$ -FDG administration
Blood glucose level	Preferably $<7$ mmol/L; $<11$ mmol/L for diabetic patients
GC interference	Delay therapy until after PET (unless risk of ischemic complications) Optional: PET within 3 d after start of GCs
PET acquisition	Positioning: supine, arms next to body Range: vertex down to feet (or at least including knees) Incubation time: standard, 60 min; optional, 120 min PET/CT: low-dose, non-contrast-enhanced CT for attenuation correction and anatomic reference Optional: diagnostic contrast-enhanced CT(A) according to local protocols and guidelines Optional: 5 min per bed position for skull only

systems, such as digital or total-body systems, may enhance sensitivity and spatial resolution with a better signal-to-noise (i.e., vessel wall vs. lumen) ratio, including the possibility to scan at later time points while retaining adequate image quality. Furthermore, these new-generation PET/CT scanners allow administration of lower tracer activities to patients while achieving similar or even better image quality than conventional scanners. These systems, including the new-generation PET/MRI scanners, may also visualize pathologic uptake in the smaller cranial vessels (e.g., temporal and vertebral arteries) (20,52). PET/MRI will further reduce the radiation dose, because CT lacks comparable accuracy in GCA diagnosis (53), and it has the advantage of tissue characterization of GCA and PMR, which is of particular value in younger individuals and in (repetitive) monitoring of disease activity (54,55).

Combining total-body systems with more specific immuno-PET tracers for vasculitis would allow more thorough insight into how specific cell subpopulations are involved and behave in the pathogenesis of specific types of vasculitis. Moreover, multiorgan changes regarding kinetic uptake of specific PET tracers after appropriate treatment of vasculitis could be assessed with total-body systems, something that was not possible before the development of this type of scanner (56).

Immuno-PET tracers, binding to specific immune cell subsets, could potentially be more accurate than conventional <sup>18</sup>F-FDG for treatment monitoring of patients with LV-GCA (57,58). However, further understanding regarding immune cell subsets in vasculitic lesions is needed for better selection of tracers and targets for tracer development.

Future studies are also needed to investigate the role of <sup>18</sup>F-FDG PET/CT in treatment monitoring and as a prognostic factor for LVV and PMR. For instance, studies have suggested that aortic <sup>18</sup>F-FDG uptake at diagnosis is associated with an enhanced risk for development of aortic aneurysms many years thereafter (59). Decision-making is always needed in the clinical context. When more specific immuno-PET tracers become available, the question may arise whether therapy should or can be modified based solely on imaging results and whether distinct immunosuppressive treatments have an equal effect on vascular uptake in patients with LVV.

In conclusion, <sup>18</sup>F-FDG PET/CT is an important diagnostic tool for detecting inflammation of large- and medium-sized vessels in patients with systemic vasculitides and in PMR. <sup>18</sup>F-FDG PET/CT can provide complementary information to other conventional imaging techniques. Furthermore, <sup>18</sup>F-FDG PET/CT may have a role in therapeutic monitoring of patients with vasculitis and PMR, but it remains challenging to differentiate remission from smoldering disease activity. A new generation of total-body PET scanners can limit radiation exposure while providing excellent sensitivity. The introduction of immune-cell targeted radiotracers will potentially allow direct visualization of inflammatory cell infiltrates in the vasculature of patients with vasculitis.

## REFERENCES

1. Jennette JC, Falk RJ, Bacon PA, et al. 2012 Revised International Chapel Hill Consensus Conference Nomenclature of Vasculitides. *Arthritis Rheum.* 2013;65:1–11.
2. Crowson CS, Matteson EL, Myasoedova E, et al. The lifetime risk of adult-onset rheumatoid arthritis and other inflammatory autoimmune rheumatic diseases. *Arthritis Rheum.* 2011;63:633–639.
3. Watts RA, Robson J. Introduction, epidemiology and classification of vasculitis. *Best Pract Res Clin Rheumatol.* 2018;32:3–20.
4. van der Geest KSM, Sandovici M, van Sleen Y, et al. Review: what is the current evidence for disease subsets in giant cell arteritis? *Arthritis Rheumatol.* 2018;70:1366–1376.

5. Mackie SL, Koduri G, Hill CL, et al. Accuracy of musculoskeletal imaging for the diagnosis of polymyalgia rheumatica: systematic review. *RMD Open.* 2015;1:e000100.
6. Jiemy WF, Zhang A, Boots AMH, et al. Expression of interleukin-6 in synovial tissue of patients with polymyalgia rheumatica. *Ann Rheum Dis.* 2023;82:440–442.
7. van der Geest KSM, Sandovici M, Brouwer E, Mackie SL. Diagnostic accuracy of symptoms, physical signs, and laboratory tests for giant cell arteritis: a systematic review and meta-analysis. *JAMA Intern Med.* 2020;180:1295–1304.
8. Soriano A, Muratore F, Pipitone N, Boiardi L, Cimino L, Salvarani C. Visual loss and other cranial ischaemic complications in giant cell arteritis. *Nat Rev Rheumatol.* 2017;13:476–484.
9. Nielsen BD, Hansen IT, Keller KK, Therkildsen P, Gormsen LC, Hauge E-M. Diagnostic accuracy of ultrasound for detecting large-vessel giant cell arteritis using FDG PET/CT as the reference. *Rheumatology.* 2020;59:2062–2073.
10. Ponte C, Grayson PC, Robson JC, et al. 2022 American College of Rheumatology/EULAR classification criteria for giant cell arteritis. *Ann Rheum Dis.* 2022;81:1647–1653.
11. Koster MJ, Warrington KJ. Classification of large vessel vasculitis: can we separate giant cell arteritis from Takayasu arteritis? *Presse Med.* 2017;46:e205–e213.
12. DeJaco C, Ramiro S, Duftner C, et al. EULAR recommendations for the use of imaging in large vessel vasculitis in clinical practice. *Ann Rheum Dis.* 2018;77:636–643.
13. Fruth M, Seggewiss A, Kozik J, Martin-Seidel P, Baraliakos X, Braun J. Diagnostic capability of contrast-enhanced pelvic girdle magnetic resonance imaging in polymyalgia rheumatica. *Rheumatology.* 2020;59:2864–2871.
14. Mackie SL, Pease CT, Fukuba E, et al. Whole-body MRI of patients with polymyalgia rheumatica identifies a distinct subset with complete patient-reported response to glucocorticoids. *Ann Rheum Dis.* 2015;74:2188–2192.
15. Dasgupta B, Cimmino MA, Kremers HM, et al. 2012 international classification criteria for polymyalgia rheumatica: a European League Against Rheumatism/American College of Rheumatology collaborative initiative. *Arthritis Rheum.* 2012;64:943–954.
16. Hellmich B, Agueda A, Monti S, et al. 2018 update of the EULAR recommendations for the management of large vessel vasculitis. *Ann Rheum Dis.* 2020;79:19–30.
17. Barra L, Yang G, Pagnoux C. Non-glucocorticoid drugs for the treatment of Takayasu's arteritis: a systematic review and meta-analysis. *Autoimmun Rev.* 2018;17:683–693.
18. Maz M, Chung SA, Abril A, et al. 2021 American College of Rheumatology/Vasculitis Foundation guideline for the management of giant cell arteritis and Takayasu arteritis. *Arthritis Rheumatol.* 2021;73:1349–1365.
19. DeJaco C, Singh YP, Perel P, et al. Current evidence for therapeutic interventions and prognostic factors in polymyalgia rheumatica: a systematic literature review informing the 2015 European League Against Rheumatism/American College of Rheumatology recommendations for the management of polymyalgia rheumatica. *Ann Rheum Dis.* 2015;74:1808–1817.
20. Nienhuis PH, Sandovici M, Glaudemans AW, Slart RH, Brouwer E. Visual and semiquantitative assessment of cranial artery inflammation with FDG-PET/CT in giant cell arteritis. *Semin Arthritis Rheum.* 2020;50:616–623.
21. Nielsen BD, Hansen IT, Kramer S, et al. Simple dichotomous assessment of cranial artery inflammation by conventional <sup>18</sup>F-FDG PET/CT shows high accuracy for the diagnosis of giant cell arteritis: a case-control study. *Eur J Nucl Med Mol Imaging.* 2019;46:184–193.
22. Blockmans D, Bley T, Schmidt W. Imaging for large-vessel vasculitis. *Curr Opin Rheumatol.* 2009;21:19–28.
23. Besson FL, Parienti J-J, Bienvenu B, et al. Diagnostic performance of <sup>18</sup>F-fluorodeoxyglucose positron emission tomography in giant cell arteritis: a systematic review and meta-analysis. *Eur J Nucl Med Mol Imaging.* 2011;38:1764–1772.
24. van der Geest KSM, Treglia G, Glaudemans AWJM, et al. Diagnostic value of [<sup>18</sup>F]FDG-PET/CT for treatment monitoring in large vessel vasculitis: a systematic review and meta-analysis. *Eur J Nucl Med Mol Imaging.* 2021;48:3886–3902.
25. Barra L, Kanji T, Malette J, Pagnoux C. Imaging modalities for the diagnosis and disease activity assessment of Takayasu's arteritis: a systematic review and meta-analysis. *Autoimmun Rev.* 2018;17:175–187.
26. Thibault T, Durand-Bailloud B, Soudry-Faure A, et al. PET/CT of cranial arteries for a sensitive diagnosis of giant cell arteritis. *Rheumatology.* July 22, 2022 [Epub ahead of print].
27. Espitia O, Blonz G, Urbanski G, et al. Symptomatic aortitis at giant cell arteritis diagnosis: a prognostic factor of aortic event. *Arthritis Res Ther.* 2021;23:14.
28. Yabusaki S, Oyama-Manabe N, Manabe O, et al. Characteristics of immunoglobulin G4-related aortitis/periarteritis and periarteritis on fluorodeoxyglucose positron emission tomography/computed tomography co-registered with contrast-enhanced computed tomography. *EJNMMI Res.* 2017;7:20.
29. Barwick TD, Lyons OTA, Mikhael NG, Waltham M, O'Doherty MJ. <sup>18</sup>F-FDG PET-CT uptake is a feature of both normal diameter and aneurysmal aortic wall and is not related to aneurysm size. *Eur J Nucl Med Mol Imaging.* 2014;41:2310–2318.

30. Treglia G, Stefanelli A, Mattoli MV, Leccisotti L, Muoio B, Bertagna F. Usefulness of <sup>18</sup>F-FDG PET/CT in evaluating disease activity at different times in a patient with chronic periaortitis. *Nucl Med Mol Imaging*. 2013;47:69–71.
31. van der Geest KSM, Treglia G, Glaudemans AWJM, et al. Diagnostic value of [<sup>18</sup>F]FDG-PET/CT in polymyalgia rheumatica: a systematic review and meta-analysis. *Eur J Nucl Med Mol Imaging*. 2021;48:1876–1889.
32. Kermani TA, Warrington KJ, Cuthbertson D, et al. Disease relapses among patients with giant cell arteritis: a prospective, longitudinal cohort study. *J Rheumatol*. 2015;42:1213–1217.
33. Slart RHJA, Slart RHJA, Glaudemans AWJM, et al. FDG-PET/CT(A) imaging in large vessel vasculitis and polymyalgia rheumatica: joint procedural recommendation of the EANM, SNMMI, and the PET Interest Group (PIG), and endorsed by the ASNC. *Eur J Nucl Med Mol Imaging*. 2018;45:1250–1269.
34. Nielsen BD, Gormsen LC, Hansen IT, Keller KK, Therkildsen P, Hauge E-M. Three days of high-dose glucocorticoid treatment attenuates large-vessel <sup>18</sup>F-FDG uptake in large-vessel giant cell arteritis but with a limited impact on diagnostic accuracy. *Eur J Nucl Med Mol Imaging*. 2018;45:1119–1128.
35. Quinn KA, Ahlman MA, Malayeri AA, et al. Comparison of magnetic resonance angiography and <sup>18</sup>F-fluorodeoxyglucose positron emission tomography in large-vessel vasculitis. *Ann Rheum Dis*. 2018;77:1165–1171.
36. Galli E, Muratore F, Mancuso P, et al. The role of PET/CT in disease activity assessment in patients with large vessel vasculitis. *Rheumatology*. 2022;61:4809–4816.
37. Schönau V, Roth J, Tascilar K, et al. Resolution of vascular inflammation in patients with new-onset giant cell arteritis: data from the RIGA study. *Rheumatology*. 2021;60:3851–3861.
38. Charpentier A, Verhoeven F, Sondag M, Guillot X, Prati C, Wendling D. Therapeutic response to prednisone in relation to age in polymyalgia rheumatica: a comparison study. *Clin Rheumatol*. 2018;37:819–823.
39. Palard-Novello X, Querellou S, Gouillou M, et al. Value of (18)F-FDG PET/CT for therapeutic assessment of patients with polymyalgia rheumatica receiving tocilizumab as first-line treatment. *Eur J Nucl Med Mol Imaging*. 2016;43:773–779.
40. Quinn KA, Rosenblum JS, Rimland CA, Gribbons KB, Ahlman MA, Grayson PC. Imaging acquisition technique influences interpretation of positron emission tomography vascular activity in large-vessel vasculitis. *Semin Arthritis Rheum*. 2020;50:71–76.
41. Gheysens O, Jamar F, Glaudemans AWJM, Yildiz H, van der Geest KSM. Semi-quantitative and quantitative [<sup>18</sup>F]FDG-PET/CT indices for diagnosing large vessel vasculitis: a critical review. *Diagnostics (Basel)*. 2021;11:2355.
42. Grayson PC, Alehashemi S, Bagheri AA, et al. 18 F-fluorodeoxyglucose-positron emission tomography as an imaging biomarker in a prospective, longitudinal cohort of patients with large vessel vasculitis. *Arthritis Rheumatol*. 2018;70:439–449.
43. Prieto Peña D, Martínez-Rodríguez I, Atienza-Mateo B, et al. Evidence for uncoupling of clinical and 18-FDG activity of PET/CT scan improvement in tocilizumab-treated patients with large-vessel giant cell arteritis. *Clin Exp Rheumatol*. 2021;39(suppl 129):S69–S75.
44. Henckaerts L, Gheysens O, Vanderschueren S, Goffin K, Blockmans D. Use of <sup>18</sup>F-fluorodeoxyglucose positron emission tomography in the diagnosis of polymyalgia rheumatica: a prospective study of 99 patients. *Rheumatology*. 2018;57:1908–1916.
45. van der Geest KSM, van Sleen Y, Nienhuis P, et al. Comparison and validation of FDG-PET/CT scores for polymyalgia rheumatica. *Rheumatology*. 2022;61:1072–1082.
46. Moreel L, Boeckxstaens L, Betrains A, et al. Diagnostic accuracy and validation of <sup>18</sup>F-fluorodeoxyglucose positron emission tomography scores in a large cohort of patients with polymyalgia rheumatica. *Front Med*. 2022;9:1026944.
47. Rabkin Z, Israel O, Keidar Z. Do hyperglycemia and diabetes affect the incidence of false-negative <sup>18</sup>F-FDG PET/CT studies in patients evaluated for infection or inflammation and cancer? A comparative analysis. *J Nucl Med*. 2010;51:1015–1020.
48. Buceri J, Mani V, Moncrieff C, et al. Optimizing <sup>18</sup>F-FDG PET/CT imaging of vessel wall inflammation: the impact of <sup>18</sup>F-FDG circulation time, injected dose, uptake parameters, and fasting blood glucose levels. *Eur J Nucl Med Mol Imaging*. 2014;41:369–383.
49. Stellingwerff MD, Brouwer E, Lensen K-JDF, et al. Different scoring methods of FDG PET/CT in giant cell arteritis: need for standardization. *Medicine (Baltimore)*. 2015;94:e1542.
50. Nienhuis PH, van Praagh GD, Glaudemans AWJM, Brouwer E, Slart RHJA. A review on the value of imaging in differentiating between large vessel vasculitis and atherosclerosis. *J Pers Med*. 2021;11:236.
51. Youngstein T, Tombetti E, Mukherjee J, et al. FDG uptake by prosthetic arterial grafts in large vessel vasculitis is not specific for active disease. *JACC Cardiovasc Imaging*. 2017;10:1042–1052.
52. Nienhuis PH, van Sluis J, van Snick JH, et al. A case of clinical uncertainty solved: giant cell arteritis with polymyalgia rheumatica swiftly diagnosed with long axial field of view PET. *Diagnostics (Basel)*. 2022;12:2694.
53. Einspieler I, Thürmel K, Pyka T, et al. Imaging large vessel vasculitis with fully integrated PET/MRI: a pilot study. *Eur J Nucl Med Mol Imaging*. 2015;42:1012–1024.
54. Young V, Khalsa U, Balboni I, Nadel H. PET/MR findings in large vessel vasculitis in children. *J Nucl Med*. 2020;61(suppl 1):1584.
55. Clemente G, de Souza AW, Leão Filho H, et al. Does [<sup>18</sup>F]F-FDG-PET/MRI add metabolic information to magnetic resonance image in childhood-onset Takayasu's arteritis patients? A multicenter case series. *Adv Rheumatol*. 2022;62:28.
56. Slart RHJA, Tsoumpas C, Glaudemans AWJM, et al. Long axial field of view PET scanners: a road map to implementation and new possibilities. *Eur J Nucl Med Mol Imaging*. 2021;48:4236–4245.
57. van der Geest KSM, Sandovici M, Nienhuis PH, et al. Novel PET imaging of inflammatory targets and cells for the diagnosis and monitoring of giant cell arteritis and polymyalgia rheumatica. *Front Med (Lausanne)*. 2022;9:902155.
58. Jiemy WF, Heeringa P, Kamps JAAM, van der Laken CJ, Slart RHJA, Brouwer E. Positron emission tomography (PET) and single photon emission computed tomography (SPECT) imaging of macrophages in large vessel vasculitis: current status and future prospects. *Autoimmun Rev*. 2018;17:715–726.
59. Tomelleri A, van der Geest KSM, Sebastian A, et al. Disease stratification in giant cell arteritis to reduce relapses and prevent long-term vascular damage. *Lancet Rheumatol*. 2021;3:e886–e895.